



1

2 **Analytical model for coupled multispecies advective-**
3 **dispersive transport subject to rate-limited sorption**

4

5

6 *Jui-Sheng Chen*^a, *Yo-Chieh Ho*^a, *Ching-Ping Liang*^b, *Sheng-Wei Wang*^c, *Chen-*

7

Wuing Liu^{d,*}

8

^a *Graduate Institute of Applied Geology, National Central University, Taoyuan City*

9

320, Taiwan

10

^b *Department of Nursing, Fooyin University, Kaohsiung City 831, Taiwan*

11

^c *Sinotech Environmental Technology, Ltd, Taipei 105, Taiwan*

12

^d *Department of Bioenvironmental Systems Engineering, National Taiwan University,*

13

Taipei 10617, Taiwan

14

15

16 **Corresponding author: Chen-Wuing Liu, Department of Bioenvironmental Systems*

17

Engineering, National Taiwan University, Taipei City 10617, Taiwan

18

E-mail: lcw901015@gmail.com

19

Tel: 886-2-23626480

20

Fax: 886-2-23639557

21

22

23

24



25 Abstract

26 Mathematical models that analytically solve a set of simultaneous multispecies
27 advection-dispersion transport equations coupled with a series of chemical reactions
28 are cost-effective tools for predicting the plume migration of dissolved chlorinated
29 solvents and nitrogen chains. However, few analytical solutions for coupled reactive
30 multispecies transport equations have appeared in the literature. For convenience of
31 mathematical derivation, most analytical models currently used to simulate
32 multispecies transport assume instantaneous equilibrium between the dissolved and
33 sorbed phases of the contaminant. However, research has demonstrated that rate-limited
34 sorption process can have a profound effect upon solute transport in the subsurface
35 environment. Making the instantaneous equilibrium sorption assumption precludes
36 consideration of potential effects of the rate-limited sorption. This study presents a
37 novel analytical model for simulating the migrations of plumes of decaying or
38 degradable contaminants subject to rate-limited sorption. The derived analytical model
39 is then applied to investigate the effects of the rate-limited sorption on the plume
40 migration of degradable contaminants. Results show that the kinetic sorption rate
41 constant has significant impacts on the plume migration of degradable contaminants.
42 Increasing the kinetic sorption rate constant results in a reduction of predicted
43 concentration for all species in the degradable contaminants while the equilibrium-
44 controlled sorption model lead to significant underestimation of the concentrations of
45 degradable contaminants under conditions with low sorption Damköler number,
46 $Da_i = \frac{\beta_i L}{v}$. The equilibrium-controlled sorption model agrees well with the rate-
47 limited sorption model when the Damköler number is greater than 2 to 3 order of
48 magnitude. The invalidity of the equilibrium-controlled sorption model of low



49 Damköler number case implies that the health risk could be underestimated if such a
50 model is used for assessing the concentrations of the degradable contaminants in the
51 health risk model.

52 **Keywords: analytical model; multispecies transport; equilibrium-controlled**
53 **sorption; rate-limited sorption, sorption reaction rate constant, Damköler number**

54

55

56

57

58

59

60

61

62

63

64

65

66

67



68 **1. Introduction**

69 Given growing concern and recognition of the potential threat of environmental
70 contaminants to human health, researchers are placing emphasis on understanding the
71 fate and transport of contaminants dissolved in the groundwater system. Study of
72 contaminant transport problems requires the use of appropriate modeling tools.
73 Mathematical models that apply analytical or numerical approaches to solve the
74 advection-dispersion equations (ADEs) have been demonstrated to be effective for
75 comprehending the transport behavior of contaminants in subsurface environments.
76 Analytical modelling is an essential and efficient tool with a variety of applications,
77 such as testing and validating numerical formulations, providing approximate analysis
78 of pollution threat scenarios, performing sensitivity analysis to investigate how various
79 parameters affect the processes of contaminant transport, extrapolating results over
80 large times or extensive spatial scales and last but not least, as a screening tool. A
81 number of analytical models has been derived for describing single-species transport of
82 various contaminants (Batu, 1989, 1993, 1996; Chen et al., 2008a, b; 2011a, b; 2016b,
83 2017; Chen and Liu, 2011; Gao et al., 2010, 2012, 2013; Leij et al., 1991, 1993; Liang
84 et al., 2016; Park and Zhan, 2001; Pérez Guerrero and Skaggs, 2010; Pérez Guerrero et
85 al., 2013; van Genuchten and Alves, 1982; Yeh, 1981; Zhan et al., 2009). However, the
86 transport processes for some contaminants of concern such as radionuclides,
87 nitrogenous and dissolved chlorinated solvents generally involve a more complicated
88 series of first-order or pseudo first-order decay or degradation chain reactions which
89 also play a decisive role affecting the migration of those decaying or degradable
90 contaminants.

91 Single-species transport analytical models are unable to account for mass



92 transformation from the parent species to the daughter species of degradable
93 contaminants. Efforts to develop multispecies transport analytical models are required
94 in order to more accurately evaluate the process of monitored natural attenuation (MNA)
95 of chlorinated solvent contaminated site. However, at the present time, only a small
96 number of multispecies transport analytical models can be found in the literature as
97 compared to the large number of single-species transport analytical models although
98 significant contributions have been made to develop multispecies transport analytical
99 models over the past decades (Chen et al., 2012a, b, 2016a; Cho, 1971; Clement, 2001;
100 Lunn et al., 1996; Mieleles and Zhan, 2012; Pérez Guerrero et al., 2009, 2010; Quezada
101 et al., 2004; Srinivasan and Clement, 2008a, b; Sudicky et al., 2013; Sun and Clement,
102 1999; Sun et al., 1999a, b; van Genuchten, 1985). Currently, all these multispecies
103 transport analytical models have been derived by considering equilibrium-controlled
104 sorption process. By making the equilibrium-controlled assumption, the rate of mass
105 adsorption and desorption between the dissolved and sorbed phases is considered to
106 occur rapidly in comparison to the time-scale required for the movement of
107 contaminants through a porous medium. When the sorption process is not sufficiently
108 fast compared to the time-scale required for transport in the dissolved phase, the
109 sorption behavior should be described as a rate-limited process.

110 It has been shown that rate-limited sorption process can have a profound effect on
111 the transport behaviors of the sorbing contaminants (van Genuchten and Wierenga,
112 1976; Nkedi-Kizza et al., 1982; Goltz and Roberts, 1988; Ball, 1989; Brusseau and Rao,
113 1989). Brusseau et al. (1991) sought to understand the influence of rate-limited sorption
114 and nonequilibrium transport on the movement of hydrophobic organic chemicals in
115 various low-organic carbon aquifer materials. Their results showed that contaminants



116 moving in a slowly flowing natural groundwater system could be successfully
117 simulated with the equilibrium-controlled sorption model. However, appropriate
118 models based on nonequilibrium or rate-limited sorption processes are needed for cases
119 when the pore water velocity is so fast that local instantaneous equilibrium cannot be
120 attained to correctly predict the solute transport behavior. Goltz and Oxley (1991)
121 demonstrated that rate-limited sorption has a significant impact upon the efficiency of
122 aquifer decontamination by pumping. The use of a rate-limited sorption model can be
123 very different from the results obtained from the equilibrium-controlled sorption model
124 in predicting contaminant concentrations and remediation time (Haggerty and Gorelick,
125 1994). Clement et al. (2004) also pointed out that the commonly used equilibrium-
126 controlled sorption approach might not be valid in some environmental assessment
127 cases. They considered a rate-limited sorption approach to simulate more realistic
128 multispecies reactive transport using the three-dimensional code RT3D (Clement,
129 1997).

130 The above review suggests that it is urgent to develop an advanced multispecies
131 reactive transport analytical model to cope with more complicated sorption process in
132 the subsurface system. To the best of our knowledge, a multispecies transport analytical
133 model subject to rate-limited sorption has not yet been developed. Thus, the objective
134 of this study is to develop a novel analytical model for describing multispecies reactive
135 transport subject to rate-limited sorption. A set of first-order reversible kinetic reaction
136 equations that represents the rate-limited sorption process between the dissolved and
137 sorbed phases of each individual species are coupled to a set of simultaneous advection-
138 dispersion transport equations. The key feature of this work is that the sorption
139 mechanisms of each individual species is considered as first-order reversible kinetic



140 rather than equilibrium-controlled. The correctness of the derived analytical models is
141 verified by comparisons of the computational results with those obtained from the
142 multispecies transport analytical model subject to equilibrium-controlled sorption and
143 numerical models for solving the same governing equations using the Laplace
144 transform finite difference (LTFD) method (Moridis and Reddell, 1991). The derived
145 analytical model is then applied to investigate the effects of the rate-limited sorption on
146 the multispecies transport of degradable contaminants. Note that the analytical
147 solutions with concise expressions are obtained by assuming that degradation reactions
148 only occur in the dissolved phase. Thus, the application of the derived analytical model
149 should consider and evaluate if the degradation reactions of the concerned degradable
150 contaminants occur only in the dissolved phase.

151

152 **2. Development of a multispecies analytical model**

153 This study considers the multispecies transport of decaying or degradable
154 contaminants subject to rate-limited sorption. The contaminant source considered is
155 chlorinated solvents dissolved into the aqueous phase from a residual non-aqueous
156 phase liquid (NAPL). After the contaminants enter the dissolved phase, transport is
157 controlled by the movement of the groundwater flow, hydrodynamic dispersion, as well
158 as the degradation reaction and the rate-limited sorption. On the microscopic scale,
159 sorption refers to the exchange of contaminants between the dissolved and sorbed
160 phases. Instead of the widely used equilibrium-controlled sorption assumption, this
161 study considers rate-limited (nonequilibrium-controlled) sorption. The rate-limited
162 sorption process is often represented as a first-order reversible kinetic reaction. When
163 dissolved contaminants migrate in the groundwater flow system, there is a loss of



164 contaminant mass in the dissolved phase due to the degradation reactions and rate-
 165 limited sorption. One key feature of the so-called multispecies model is that the mass
 166 accumulation of the predecessors is also considered. Based on the conceptual
 167 description, the governing equations for describing one-dimensional transport of
 168 degradable contaminants involving an arbitrary number of species undergoing a series
 169 of first-order degradation reactions in the dissolved phase and first-order reversible
 170 kinetic sorption reaction between the dissolved and sorbed phases are

$$171 \quad D \frac{\partial^2 C_1(x,t)}{\partial x^2} - v \frac{\partial C_1(x,t)}{\partial x} - \lambda_1 C_1(x,t) - \frac{\beta_1}{\theta} \left(C_1(x,t) - \frac{S_1(x,t)}{K_1} \right) = \frac{\partial C_1(x,t)}{\partial t} \quad (1a)$$

$$172 \quad D \frac{\partial^2 C_i(x,t)}{\partial x^2} - v \frac{\partial C_i(x,t)}{\partial x} - \lambda_i C_i(x,t) + \lambda_{i-1} C_{i-1}(x,t) - \frac{\beta_i}{\theta} \left(C_i(x,t) - \frac{S_i(x,t)}{K_i} \right) = \frac{\partial C_i(x,t)}{\partial t} \quad i = 2, \dots, N \quad (1b)$$

$$173 \quad \rho_b \frac{\partial S_i(x,t)}{\partial t} = \beta_i \left(C_i(x,t) - \frac{S_i(x,t)}{K_i} \right) \quad i = 1, \dots, N \quad (2)$$

174 where $C_i(x,t)$ is the concentration of species i in the dissolved phase [ML^{-3}]; $S_i(x,t)$
 175 is the concentration of species i in the sorbed phase [MM^{-1}]; v is the average uniform
 176 pore-water velocity [LT^{-1}]; D is the hydrodynamic dispersion coefficient [L^2T^{-1}]; x
 177 is the spatial coordinate [L]; t is the time [T]; θ is the porosity; ρ_b is the bulk dry
 178 density of the solid grain [ML^{-3}]; K_i is the distribution coefficient of species i [M^{-1}L^3];
 179 λ_i is the first-order degradation rate constant of species i in the dissolved phase [T^{-1}];
 180 β_i is the first-order sorption rate constant of species i between the dissolved and



181 sorbed phases [T^{-1}] (referred to as the kinetic sorption rate constant thereafter); N is the
182 total species number of degradable contaminants. Eqs. (1a) and (1b) describe the
183 advective-dispersive transport of the dissolved phase of degradable contaminants
184 subject to a series of first-order degradation reactions and first-order reversible kinetic
185 (rate-limited) mass transfer due to sorption. The mass transfer between the dissolved
186 and sorbed phases of multiple species is represented by a first-order reversible kinetic
187 reaction coupled to the equations so that the assumption of rate-limited sorption can be
188 considered. Eq. (2) accounts for mass conservation in the sorbed phase of multiple
189 species. Note that these equations consider that the degradation reactions occur only in
190 both the dissolved phase. The fourth term on the left-hand side of Eq. (1a) and the fifth
191 term on the left-hand side of Eq. (1b) quantify the mass accumulation from the
192 predecessor species between the dissolved and sorbed phases. The above coupled
193 equations described in Eqs. (1a), (1b) and (2) must be solved simultaneously to obtain
194 the solutions for each individual species in the dissolved and sorbed phases. It should
195 be pointed out that, for the sake of clarity, the porous medium is considered
196 homogeneous and all the aforementioned transport parameters of the porous medium
197 are assumed to be independent of time and space.

198 The medium is initially assumed to be free of the individual species mass of a
199 decay chain in both the dissolved and sorbed phases:

$$200 \quad C_i(x, t = 0) = 0 \quad i = 1, \dots, N \quad (3)$$

$$201 \quad S_i(x, t = 0) = 0 \quad i = 1, \dots, N \quad (4)$$

202 There is assumed to be a continuous constant concentration of dissolved phase
203 contaminant sources. The contaminant sources are treated mathematically as third-type
204 boundary conditions and formulated as



$$205 \quad -D \frac{\partial C_i(x=0,t)}{\partial x} + vC_i(x=0,t) = vc_{i,0} \quad i = 1, \dots, N \quad (5)$$

206 where $c_{i,0}$ is the source of the constant concentration of species i at the inlet boundary
 207 [ML⁻³]. The third-type boundary conditions in Eq. (5) is regarded as satisfying the
 208 principle of mass conservation of each individual species at the inlet boundary. A finite-
 209 domain subsurface porous medium system is considered in this study. Considering the
 210 mass conservation of each individual species at the outlet boundary, a second-type
 211 boundary condition with zero concentration gradient is used and can be mathematically
 212 expressed as

$$213 \quad \frac{\partial C_i(x=L,t)}{\partial x} = 0 \quad i = 1, \dots, N \quad (6)$$

214 where L is the length of the transport system [L].

215 The derivation of the analytical solutions to the initial-boundary value problems
 216 as defined in Eqs. (1a), (1b) and (2)-(6) is facilitated by reducing the number of model
 217 parameters. The coupled governing equations, initial conditions and boundary
 218 conditions are transformed into dimensionless forms as follows:

$$219 \quad \frac{1}{Pe} \frac{\partial C_1^2(X,T)}{\partial X^2} - \frac{\partial C_1(X,T)}{\partial X} - \Lambda_1 C_1(X,T) - \frac{B_1}{\theta} \left(C_1(X,T) - \frac{S_1(X,T)}{K_1} \right) = \frac{\partial C_1(X,T)}{\partial T} \quad i = 2, \dots, N \quad (6a)$$

$$220 \quad \frac{1}{Pe} \frac{\partial^2 C_i(X,T)}{\partial X^2} - \frac{\partial C_i(X,T)}{\partial X} - \Lambda_i C_i(X,T) + \Lambda_{i-1} C_{i-1}(X,T) - \frac{B_i}{\theta} \left(C_i(X,T) - \frac{S_i(X,T)}{K_i} \right) = \frac{\partial C_i(X,T)}{\partial T} \quad (6b)$$



$$221 \quad K_i \rho_b \frac{\partial S_i(X, T)}{\partial T} = B_i (K_i C_i(X, T) - S_i(X, T)) \quad i = 1, \dots, N \quad (7)$$

$$222 \quad C_i(X, T = 0) = 0 \quad i = 1, \dots, N \quad (8)$$

$$223 \quad S_i(X, T = 0) = 0 \quad i = 1, \dots, N \quad (9)$$

$$224 \quad -\frac{1}{Pe} \frac{\partial C_i(X=0, T)}{\partial X} + C_i(X=0, T) = c_{i,0} \quad i = 1, \dots, N \quad (10)$$

$$225 \quad \frac{\partial C_i(X=1, T)}{\partial X} = 0 \quad i = 1, \dots, N \quad (11)$$

$$226 \quad \text{where } X = \frac{x}{L}, \quad T = \frac{vt}{L}, \quad Pe = \frac{vL}{D}, \quad \Lambda_i = \frac{\lambda_i L}{v}, \quad B_i = \frac{\beta_i L}{v}, \quad \Gamma_i = \frac{\gamma_i L}{v}.$$

227 The solution strategy adopted in this study is an extension of an efficient method
 228 for analytically solving a set of coupled advection-dispersion equations proposed by
 229 Chen et al. (2012a).

230 The first step is to take the Laplace transform with respect to T . After the
 231 Laplace transform, Eqs. (6a), (6b) and (7) can be expressed as

$$232 \quad \frac{1}{Pe} \frac{d^2 C_1^L(X, s)}{dX^2} - \frac{dC_1^L(X, s)}{dX} - \Lambda_1 C_1^L(X, s) - \frac{B_1}{\theta} \left(C_1^L(X, s) - \frac{S_1^L(X, s)}{K_1} - s C_1^L(X, s) \right) = 0 \quad (12a)$$

$$233 \quad \frac{1}{Pe} \frac{d^2 C_i^L(X, s)}{dX^2} - \frac{dC_i^L(X, s)}{dX} - \Lambda_i C_i^L(X, s) + \Lambda_{i-1} C_{i-1}^L(X, s) - \frac{B_i}{\theta} \left(C_i^L(X, s) - \frac{S_i^L(X, s)}{K_i} - s C_i^L(X, s) \right) = 0 \quad i = 2, \dots, N \quad (12b)$$

$$234 \quad s K_i \rho_b S_i^L(X, s) = B_i (K_i C_i^L(X, s) - S_i^L(X, s)) \quad (13)$$



235 where $C_i^L(X, s) = \int_0^\infty e^{-sT} C_i(X, T) dT$ and $S_i^L(X, s) = \int_0^\infty e^{-sT} S_i(X, T) dT$, s is the

236 Laplace transform parameter.

237 Then, we can solve Eq. (13) algebraically for the transform of the sorbed phase

238 concentration for each individual species ($S_i^L(X, s)$) and $S_i^L(X, s)$ is conveniently

239 expressed in terms of the transform of dissolved phase concentration for each individual

240 species ($C_i^L(X, s)$) Through substitution of the relations between $S_i^L(X, s)$

241 $C_i^L(X, s)$, Eqs. (12a) and (12b) can be expressed as

$$242 \quad \frac{1}{Pe} \frac{d^2 C_1^L(X, s)}{dX^2} - \frac{dC_1^L(X, s)}{dX} - \Theta_1(s) C_1^L(X, s) = 0 \quad (14a)$$

$$243 \quad \frac{1}{Pe} \frac{d^2 C_i^L(X, s)}{dX^2} - \frac{dC_i^L(X, s)}{dX} - \Theta_i(s) C_i^L(X, s) \quad i = 2, \dots, N \quad (14b)$$

$$= -\Lambda_{i-1} C_{i-1}^L(X, s)$$

$$244 \quad \text{where } \Theta_i(s) = s + \Lambda_i + \frac{B_i}{\theta} \frac{sK_i \rho_b}{sK_i \rho_b + B_i}.$$

245 The boundary conditions after the Laplace transform become

$$246 \quad -\frac{1}{Pe} \frac{dC_i^L(X=0, s)}{dX} + C_i^L(X=0, s) = \frac{c_{i,0}}{s} \quad i = 1, \dots, N \quad (15)$$

$$247 \quad \frac{dC_i^L(X=1, s)}{dX} = 0 \quad i = 1, \dots, N \quad (16)$$

248 Next, the integral transform technique is used to eliminate the X variable and

249 reduce the system of the ordinary differential equations into a set of linear algebraic

250 equations. Prior to applying the integral transform technique, we need to homogenize



251 the boundary condition in Eq. (15) and convert Eqs. (14a) and (14b) into purely
 252 diffusive equations. The homogenization of the boundary conditions in Eq. (15) is done
 253 with a change of variable

$$254 \quad C_i^L(X, s) = e^{\frac{Pe}{2}X} C_i^{LV}(X, s) + \frac{c_{i,0}}{s} \quad (17)$$

255 Eqs. (14a), (14b), (15) and (16) are then written as

$$256 \quad \frac{1}{Pe} \frac{d^2 C_1^{LV}(X, s)}{dX^2} - \left(\Theta_1(s) + \frac{Pe}{4} \right) C_1^{LV}(X, s) = \frac{c_{1,0}}{s} \Theta_1(s) e^{-\frac{Pe}{2}X} \quad (18a)$$

$$257 \quad \begin{aligned} & \frac{1}{Pe} \frac{d^2 C_i^{LV}(X, s)}{dX^2} - \frac{dC_i^{LV}(X, s)}{dX} - \Theta_i(s) C_i^{LV}(X, s) \\ & = \frac{c_{i,0}}{s} \Theta_i(s) e^{-\frac{Pe}{2}X} - \Lambda_{i-1} \left(C_{i-1}^{LV}(X, s) + \frac{c_{i-1,0}}{s} e^{-\frac{Pe}{2}X} \right) \end{aligned} \quad (18b)$$

$$258 \quad -\frac{dC_i^{LV}(X=0, s)}{dX} + \frac{Pe}{2} C_i^{LV}(X=0, s) = 0 \quad i = 1, \dots, N \quad (19)$$

$$259 \quad \frac{dC_i^{LV}(X=1, s)}{dX} + \frac{Pe}{2} C_i^{LV}(X=1, s) = 0 \quad i = 1, \dots, N \quad (20)$$

260 The integral transform technique for eliminating the second-order spatial
 261 derivative with respect to X is dependent on the governing equations in Eqs. (18a)
 262 and (18b) and their corresponding boundary conditions in Eqs. (19) and (20). The
 263 appropriate integral transform pairs in relation to Eqs. (18a), (18b), (19) and (20) can
 264 be found as follows (Chen et al., 2012a):

$$265 \quad G[C_i^{LV}(X, s)] = C_i^{LVG}(\psi_m, s) = \int_0^1 K(\psi_m, X) C_i^{LV}(X, s) dX \quad (21a)$$

$$266 \quad G[C_i^{LVG}(X, s)] = C_i^{LV}(X, s) = \sum_{m=1}^{\infty} N(\psi_m) K(\psi_m, X) C_i^{LVG}(\psi_m, s) \quad (21b)$$



267 where $K(\psi_m, X) = \frac{Pe}{2} \sin(\psi_m X) + \psi_m \cos(\psi_m X)$, $N(\psi_m) = \frac{2}{\frac{Pe^2}{4} + \psi_m^2}$, and

268 ψ_m is the eigenvalue determined from the following equation

269
$$\psi_m \cot \psi_m - \frac{\psi_m^2}{Pe} + \frac{Pe}{4} = 0.$$

270 The operational formula for the generalized integral transform of the second-
 271 order derivatives of $C_i^{LV}(X, s)$ satisfies

272
$$G \left[\frac{d^2 C_i^{LV}(X, s)}{dX^2} \right] = -\psi_m^2 \left[C_i^{LV}(X, s) \right] \quad (22)$$

273 Taking the integral transform operator (Eq. (21a)) on both sides of Eq. (18a) and
 274 we get

275
$$-\left(\Theta_1(s) + \frac{Pe}{4} + \frac{\psi_m^2}{Pe} \right) C_1^{LHV}(X, s) = \frac{c_{1,0}}{s} \Theta_1(s) \Phi(\psi_m) \quad (23a)$$

276
$$-\left(\Theta_i(s) + \frac{Pe}{4} + \frac{\psi_m^2}{Pe} \right) C_i^{LVG}(X, s) \quad (23b)$$

$$= \frac{c_{i,0}}{s} \Theta_i(s) \Phi(\psi_m) - \Lambda_{i-1} \left(C_{i-1}^{LVG}(X, s) + \frac{c_{i-1,0}}{s} \Phi(\psi_m) \right)$$

277 where $\Phi(\psi_m) = \frac{Pe \psi_m}{\frac{Pe^2}{4} + \psi_m^2}$.

278 Solving Eqs. (23a) and (23b) for each individual species $C_i^{LVG}(\psi_m, s)$ in
 279 sequence, we can generalize $C_i^{LVG}(\psi_m, s)$ in a compact expression as



$$C_i^{LVG}(X, s) = \left[-\frac{c_{i,0}}{s} \frac{\Theta_i(s)}{p_i(s)} + \sum_{l=1}^{i-1} \frac{c_{i-l,0}}{s} \frac{\left(\prod_{k=i-l}^{k=i-1} \Lambda_k \right) (p_{i-l}(s) - \Theta_{i-l}(s))}{\prod_{k=i-l}^{k=i} p_k(s)} \right] \Phi(\psi_m)$$

280

281

(24)

282 where $p_i(s) = \Theta_i(s) + \frac{Pe}{4} + \frac{\psi_m^2}{Pe}$.

283

284 3. Results and discussion

285 3.1 Convergence evaluation and verification of the derived analytical solution

286 The derived generalized analytical solution in Eq. (24) is mathematically
 287 expressed as the sum of an infinite series expansion. The numerical evaluation of this
 288 infinite series expansion sum can be calculated straightforwardly. To ensure the
 289 precision of the numerical evaluation, while at the same time avoiding the redundant
 290 computation of the infinite series expansion term by term, it is important to investigate
 291 the convergence behavior of the numerical evaluation of the derived analytical solutions.
 292 We executed routine convergence tests to determine the optimal number required for
 293 summing up the infinite series expansion term by term to obtain the desired accuracies.
 294 An illustrated example coming from the manual for the most commonly used public
 295 domain model BIOCHLOR provided by the Center for Subsurface Modeling Support
 296 of the United States Environmental Protection Agency (USEPA) (Aziz et al., 2000) is
 297 considered herein to evaluate the convergence of the numerical calculation of the
 298 developed analytical model. This illustrative example simulates the natural attenuation
 299 of the groundwater contaminant plumes of a chlorinated solvent site. The
 300 biodegradation pathway of the chlorinated solvent is assumed to follow sequential first-



301 order kinetics as follows: $PCE \rightarrow TCE \rightarrow DCE \rightarrow VC \rightarrow ETH$. The descriptive
302 simulation conditions and transport parameters are summarized in Table 1. Table 2
303 shows the convergence behavior obtained by the numerical evaluation of the spatial
304 concentration profiles of the five species using the derived analytical solution in Eq.
305 (24) with a desired accuracy of 2 decimal digits. In Table 2, N is defined as the number
306 required for summing up the infinite series expansion term by term. It can be seen that
307 for larger values of Pe , the evaluation must be carried out with a large number for
308 summing up the series expansion to desired accuracy of 2 decimal digits. Moreover,
309 the number required for accurately summing up the series expansion decreases as the
310 serial number of the species increases. The number of terms required for convergence
311 are 40, 1000 and 16,000 for $Pe=1, 10$ and 20 , respectively, for the PCE of the first
312 species, and 20, 320 and 2,000, respectively, for $Pe=1, 10$ and 20 for the TCE of the
313 second species. For VC of the fourth species, convergence is reached when the numbers
314 of terms are 8, 80 and 800 for $Pe=1, 10$ and 20 , while for ETH only 8, 20 and 100 terms
315 are required to meet the desired accuracy for $Pe = 1, 10$ and 20 .

316 A computer code for executing the calculation of the developed analytical model
317 is constructed based on the aforementioned convergence criterion. Comparison
318 between the computed results obtained from the computer code constructed for the
319 analytical model and the simulated results from a corresponding numerical solutions is
320 carried out to assess the correctness the derived analytical model, as well as the
321 accuracy of its auxiliary computer code. The numerical solutions are obtained using the
322 Laplace transform finite difference (LTFD) method developed by Moridis and Reddel
323 (1991) for the purpose of solving the partial differential equation for transient
324 groundwater flow through porous media. The LTFD method provides an approach to



325 solve the discretized partial differential equation in the Laplace domain and then
326 numerically invert the transformed solution vectors. Therefore, we are able to obtain a
327 solution which is only discretized in space and continuous in time. The comparative
328 example considers the same simulation conditions and transport parameters for natural
329 attenuation of the contamination plumes of a chlorinated solvent site as those used for
330 the convergence evaluation. The comparison clearly shows excellent agreement
331 between the spatial concentration distributions for all five species obtained from the
332 analytical and numerical solutions (see supporting information). The results confirm
333 the correctness of the developed analytical models as well as the accuracy and
334 usefulness of the constructed computer code.

335

336 **3.2 Effect of the kinetic sorption rate constant (β_i)**

337 The major merit of the derived analytical solution is that the sorption process can
338 be more realistically and flexibly described as a first-order reversible kinetic sorption
339 process with an important kinetic sorption rate constant (β_i). Therefore, we are
340 interested in how β_i affects the multispecies plume migration. We now consider the
341 same multispecies transport problem used in the previous convergence evaluation and
342 solution verification to investigate the effect of β_i on multispecies plume
343 development. The simulation conditions and model parameters used in the convergence
344 tests are considered as a baseline simulation. For each of the individual species i , four
345 values of β_i (0, 0.5, 5 and 50 year⁻¹) are considered in order to investigate the effect
346 of β_i on multispecies transport. Figure 1 depicts the spatial concentration profiles of
347 the five species at $t=1$ year under different β_i values. The spatial concentration



348 profiles of the five species obtained with the equilibrium-controlled linear sorption
349 model are also included in Fig. 1. It is found that an increase in β_i will lead to a
350 decrease in the peak concentration and a upstream shift in the location of the peak
351 concentration. As β_i continues to increase, the spatial concentration profile obtained
352 from the rate-limited sorption model of gradually reaches those obtained from the
353 equilibrium-controlled sorption model. The spatial concentration profiles show that the
354 rate-limited sorption model of $\beta_i = 50 \text{ year}^{-1}$ coincides with the equilibrium-controlled
355 sorption model. It further demonstrates that the asymptotical condition of the rate-
356 limited sorption model agrees with the equilibrium-controlled sorption model. The
357 higher peak concentrations predicted by the rate-limited sorption model with small β_i
358 values have important implications for groundwater contaminant concentration
359 predictions as well as the assessment of the risk to human health. It should be noted that
360 the health risk might be underestimated when an equilibrium-controlled sorption model
361 is used for assessing the exposure concentration.

362 To measure the relative importance of rate-limited sorption between the dissolved
363 and sorbed phases in comparison to advection process, the sorption Damköler number,

364 $Da_i = \frac{\beta_i L}{v}$, which is the ratio of time ($\frac{L}{v}$) taken for the groundwater moving a distance

365 L through the aquifer to the time scale for kinetic sorption rate constant β_i is
366 considered. The Da_i is a dimensionless number to relate the sorption reaction rate to
367 the advective transport rate is considered. A smaller value of Da_i indicates that the
368 sorption reaction rate between the dissolved and the sorbed phase is relatively smaller
369 in comparison to rate of the groundwater flow through a porous medium. As β_i



370 gradually increases, the Da_i increases proportionally. With coincidence between the
371 rate-limited sorption model of $\beta_i = 50y^{-1}$ and the equilibrium-controlled sorption
372 model, $Da_i = \frac{\beta_i L}{v} = \frac{50y^{-1} \times 330.7m}{34.0m/y} = 486$. is obtained. It should be noted that
373 $Da_i = 486$ for validity condition of the equilibrium-controlled sorption model is
374 obtained on our descriptive simulation conditions and transport parameters. Uncertainty
375 analysis on the value for the threshold of Da should be conducted to support the general
376 validity condition. Nevertheless, considering the valid condition of the equilibrium-
377 controlled sorption model can vary with the combinations of all the transport
378 parameters used in the modeling process, the Damköler number greater than 2 to 3 order
379 of magnitude is suggested.

380 The results of the aforementioned investigation clearly evidence that the kinetic
381 sorption rate constant is an important parameter governing the multispecies plume
382 transport. However, because of the difficulty in obtaining the sorption reaction rate
383 constant, current transport modeling practices are often based on the equilibrium
384 sorption assumption. Thus, more efforts are required to develop a method for more
385 effective and accurately determining the kinetic sorption rate coefficient in the field

386

387 **3.3 Effect of inlet boundary condition**

388 Several previous studies have discussed the mass balance constraints and potential
389 errors in concentration prediction when improper inlet boundary conditions are used
390 for the development of the single-species transport analytical model (van Genuchten
391 and Parker, 1984; Leij et al., 1991, Chen et al., 2011a; 2011b). Single-species transport



392 analytical models with a first-type inlet condition give rise to physically improper mass
393 conservation and significant errors in predicting the solute concentration distribution,
394 especially for a porous medium system with a large longitudinal dispersion coefficient
395 if it is used to interpret the usual volume-average concentration. Selection of the
396 appropriate inlet boundary condition has been the subject of much investigation, such
397 as for the study of solute transport either in a uniform flow ((van Genuchten and Parker,
398 1984; Leij et al., 1991; Chen et al. 2011a; 2011b) or a radial flow field (Chen, 1987).
399 To the best of the author's knowledge, the effect of the inlet boundary condition on
400 multispecies transport has not been investigated yet. Here, the impact of the inlet
401 boundary conditions on multispecies transport are investigated using our derived
402 multispecies transport analytical models subject to the first-type and third-type inlet
403 boundary conditions. The analytical solutions for the first-type inlet boundary
404 condition can be obtained following the same method. Chen et al. (2011b) has showed
405 how to obtain the analytical solution for single-species transport in a finite domain with
406 a first-type inlet boundary condition. Figure 2 depicts the spatial concentration profiles
407 of the five species at $t=1$ year for both the first-type and third-type inlet boundary
408 conditions. using different dispersion coefficient values. It is observed that the predicted
409 concentration is higher for the first-type inlet boundary condition than with the third-
410 type inlet boundary condition for all species. Moreover, with an increasing dispersion
411 coefficient, the discrepancy between the concentration distributions for first-type and
412 third-type inlet boundary conditions increases along with the discrepancy between the
413 peak concentrations. The results show that improper inlet boundary conditions leads to
414 pronounced mass balance errors, and the discrepancy increases as the dispersion
415 coefficient increases



416

417 **4. Conclusions**

418 In this study, a novel analytical model is developed for multispecies advective-
419 dispersive transport subject to rate-limited sorption. The developed model is then
420 applied to assess the effects of the kinetic sorption rate constant on multispecies
421 transport. Increasing the kinetic sorption rate constant leads to lower concentration
422 predictions for all species of the degradable contaminants. The equilibrium-controlled
423 sorption model could significantly underestimate the concentration of decaying or
424 degradable contaminants under the condition of a low sorption Damköler number,

425 $Da_i = \frac{\beta_i L}{v}$, but will agree well with the rate-limited sorption model when the sorption

426 Damköler number is greater than 486. It should be noted that $Da_i = 486$ for validity
427 condition of the equilibrium-controlled sorption model is obtained on our descriptive
428 simulation conditions and transport parameters. Uncertainty analysis on the value for
429 the threshold of Da should be conducted to support the general validity condition. The
430 invalidity of the equilibrium-controlled sorption model under a low sorption Damköler
431 number suggests that the health risk might be underestimated when an equilibrium-
432 controlled sorption model is used for assessing the exposure concentration in the health
433 risk assessment of the contaminated site.

434

435 **Acknowledgement**

436 The authors are grateful to the Ministry of Science and Technology, Republic of
437 China and Sinotech Environmental Technology, Ltd for financial support of this
438 research under contract MOST 106-2622-M-008-001-CC2.



439

440 **References**

441 Aziz, C. E., Newell, C. J., Gonzales, J. R., Haas P., Clement, T.P., and Sun, Y.:

442 BIOCHLOR–Natural attenuation decision support system v1.0, User’s Manual,

443 US EPA Report, EPA 600/R-00/008, 2000.

444 Ball, W. P.: Equilibrium sorption and diffusion rate studies with halogenated organic

445 chemical and sandy aquifer material, Ph.D. dissertation, pp.356, Stanford Univ.,

446 Stanford, Calif., 1989.

447 Batu, V.: A generalized two-dimensional analytical solution for hydrodynamic

448 dispersion in bounded media with the first-type boundary condition at the source.

449 Water Resour. Res., 25, 1125-1132, 1989.

450 Batu, V.: A generalized two-dimensional analytical solute transport model in bounded

451 media for flux-type finite multiple sources, Water Resour. Res., 29, 2881-2892,

452 1993.

453 Batu, V., 1996.: A generalized three-dimensional analytical solute transport model for

454 multiple rectangular first-type sources, J. Hydrol., 174, 57-82, 1996.

455 Brusseau, M. L., and Rao, P. S. C.: Sorption nonideality during organic contaminant

456 transport in porous media, CRC Crit. Rev. Environ. Control, 19(1), pp. 33-99,

457 1989.

458 Brusseau, M. L., Larsen, T., and Christensen T.H.: Rate-limited sorption and

459 nonequilibrium transport of organic chemicals in low organic carbon aquifer

460 materials, Water Resour. Res., 27(6), 1137-1145, 1991.

461 Chen, C. S.: Analytical solutions for radial dispersion with Cauchy boundary at

462 injection well., Water. Resour. Res. 23(7):1217–24, 1987.



- 463 Chen, J. S., Ni, C. F., and Liang, C. P.: Analytical power series solutions to the two-
464 dimensional advection-dispersion equation with distance-dependent
465 dispersivities, *Hydrol. Process.*, 22, 4670-4678, 2008a.
- 466 Chen, J. S., Ni, C. F., Liang, C. P., and Chiang, C. C.: Analytical power series solution
467 for contaminant transport with hyperbolic asymptotic distance-dependent
468 dispersivity, *J. Hydrol.*, 362, 142-149, 2008b.
- 469 Chen, J. S., Liu, Y. H., Liang, C. P., Liu, C. W., and Lin, C.W.: Exact analytical
470 solutions for two-dimensional advection-dispersion equation in cylindrical
471 coordinates subject to third-type inlet boundary condition, *Adv. Water Resour.*,
472 34, 365-374, 2011a.
- 473 Chen, J. S., Chen, J. T., Liu, C. W., Liang, C. P., and Lin, C. W.: Analytical solutions
474 to two-dimensional advection–dispersion equation in cylindrical coordinates in
475 finite domain subject to first- and third-type inlet boundary conditions, *J. Hydrol.*,
476 405, 522-531, 2011b.
- 477 Chen, J. S., and Liu, C. W.: Generalized analytical solution for advection-dispersion
478 equation in finite spatial domain with arbitrary time-dependent inlet boundary
479 condition, *Hydrol. Earth Syst. Sci.*, 15, 2471-2479, 2011.
- 480 Chen, J. S., Lai, K. H., Liu, C. W., and Ni, C. F.: A novel method for analytically
481 solving multi-species advective-dispersive transport equations sequentially
482 coupled with first-order decay reactions, *J. Hydrol.*, 420–421, 191-204, 2012a.
- 483 Chen, J. S., Liu, C. W., Liang, C. P., and Lai, K. H.: Generalized analytical solutions to
484 sequentially coupled multi-species advective-dispersive transport equations in a
485 finite domain subject to an arbitrary time-dependent source boundary condition.
486 *J. Hydrol.*, 456–457, 101-109, 2012b.



- 487 Chen, J. S., Liang, C. P., Liu, C. W., and Li, L. Y.: An analytical model for simulating
488 two-dimensional multispecies plume migration, *Hydrol. Earth Syst. Sci.*, 20, 733-
489 753, 2016a.
- 490 Chen, J. S., Hsu, S. Y., Li, M. H., and Liu, C. W.: Assessing the performance of a
491 permeable reactive barrier-aquifer system using a dual-domain solute transport
492 model, *J. Hydrol.*, 543, 849-860, 2016b.
- 493 Chen, J. S., Li, L. Y., Lai, K. H., and Liang, C. P.: Analytical model for advective-
494 dispersive transport involving flexible boundary inputs, initial distributions and
495 zero-order productions, *J. Hydrol.*, 554, 187-199, 2017.
- 496 Cho, C. M.: Convective transport of ammonium with nitrification in soil, *Can. J. Soil*
497 *Sci.*, 51, 339–350, 1971.
- 498 Clement, T. P., RT3D-A modular computer code for simulating reactive multi-species
499 transport in 3-dimensional groundwater aquifers, Battelle Pacific Northwest
500 National Laboratory, PNNL-SA-28967, 1997.
- 501 Clement, T. P.: Generalized solution to multispecies transport equations coupled with
502 a first-order reaction-network, *Water Resour. Res.*, 37, 157-163, 2001.
- 503 Clement, T. P., Gautam T. R., Lee, K. K., Truex, M. J., and Davis, G. B.: Modeling of
504 DNAPL-dissolution, rate-limited sorption and biodegradation reactions in
505 groundwater systems, *Biorem. J.*, 8(1-2), 47-64, 2004.
- 506 Gao, G., Zhan, H., Feng, S., Fu, B., Ma, Y., and Huang, G.: A new mobile-immobile
507 model for reactive solute transport with scale-dependent dispersion, *Water*
508 *Resour. Res.*, 46, W08533, doi:10.1029/2009WR008707, 2010.
- 509 Gao, G., Zhan, H., Feng, S., Huang, G., and Fu, B.: A mobile-immobile model with
510 an asymptotic scale-dependent dispersion function, *J. Hydrol.*, 424-425, 172-



- 511 183, 2012.
- 512 Gao, G., Fu, B., Zhan, H., and Ma, Y.: Contaminant transport in soil with depth-
513 dependent reaction coefficients and time-dependent boundary conditions, *Water*
514 *Res.*, 47, 2507-2522, 2013.
- 515 Goltz, M. N., and Roberts, P. V.: Simulations of physical solute transport models:
516 Application to a large-scale field experiment, *J. Contain. Hydrol.*, 3(1), 37-63,
517 1988.
- 518 Goltz M. N., and Oxley M. E.: Analytical modeling of aquifer decontamination by
519 pumping when transport is affected by rate-limited sorption, *Water Resour. Res.*,
520 27(4), 547-556, 1991.
- 521 Haggerty, R., and Gorelick, S. M.: Design of multiple contaminant remediation:
522 Sensitivity to rate-limited mass transfer, *Water Resour. Res.* 30, 435-446, 1994.
- 523 Leij, F. J., Skaggs, T. H., and Van Genuchten, M. T.: Analytical solution for solute
524 transport in three-dimensional semi-infinite porous media, *Water Resour. Res.*,
525 27, 2719–2733, 1991.
- 526 Leij, F. J., Toride, N., and van Genuchten, M. T.: Analytical solutions for non-
527 equilibrium solute transport in three-dimensional porous media, *J. Hydrol.*, 151,
528 193–228, 1993.
- 529 Liang, C. P., Hsu, S. Y., and Chen, J. S.: An analytical model for solute transport in an
530 infiltration tracer test in soil with a shallow groundwater table, *J. Hydrol.*, 540,
531 129-141, 2016.
- 532 Lunn, M., Lunn, R. J., and Mackay, R.: Determining analytic solution of multiple
533 species contaminant transport with sorption and decay, *J. Hydrol.*, 180, 195-210,
534 1996.



- 535 Mieleś, J. and Zhan, H.: Analytical solutions of one-dimensional multispecies reactive
536 transport in a permeable reactive barrier-aquifer system, *J. Contam. Hydrol.*, 134-
537 135, 54-68, 2012.
- 538 Moridis, G. J., and Reddell, D. L., 1991. The Laplace transform finite difference
539 method for simulation of flow through porous media, *Water Resour. Res.*, 27 (8),
540 1873-1884, 1991.
- 541 Nkedi-Kizza, P., Rao, P. S. C., Jessup, R. E. and Davidson, J. M.: Ion exchange and
542 diffusive mass transfer during miscible displacement through an aggregate oxisol,
543 *Soil Sci. Soc. Am. J.*, 46, 471-476, 1982.
- 544 Park, E. and Zhan, H.: Analytical solutions of contaminant transport from finite one-,
545 two, three-dimensional sources in a finite thickness aquifer, *J. Contam. Hydrol.*,
546 53, 41–61, 2001.
- 547 Pérez Guerrero, J. S. and Skaggs, T. H.: Analytical solution for one-dimensional
548 advection-dispersion transport equation with distance-dependent coefficients, *J.*
549 *Hydrol.*, 390, 57–65, 2010.
- 550 Pérez Guerrero, J. S., Pimentel, L. G. G., Skaggs, T. H., and van Genuchten, M. T.:
551 Analytical solution for multi-species contaminant transport subject to sequential
552 first-order decay reactions in finite media, *Transport Porous Med.*, 80, 357–373,
553 2009.
- 554 Pérez Guerrero, J. S., Skaggs, T. H., and van Genuchten, M. T.: Analytical solution for
555 multi-species contaminant transport in finite media with time-varying boundary
556 condition, *Transport Porous Med.*, 85, 171-188, 2010.
- 557 Pérez Guerrero, J. S., Pontedeiro, E. M., van Genuchten, M. T., and Skaggs, T. H.:
558 Analytical solutions of the one-dimensional advection–dispersion solute



- 559 transport equation subject to time-dependent boundary conditions, *Chem. Eng. J.*,
560 221, 487–491, 2013.
- 561 Quezada, C. R., Clement, T. P., and Lee, K. K.: Generalized solution to multi-
562 dimensional multi-species transport equations coupled with a first-order reaction
563 network involving distinct retardation factors, *Adv. Water Res.*, 27, 507–520,
564 2004.
- 565 Srinivasan, V. and Clement, T. P.: Analytical solutions for sequentially coupled one-
566 dimensional reactive transport problems - Part I: Mathematical derivations,
567 *Adv. Water Resour.*, 31, 203–218, 2008a.
- 568 Srinivasan, V. and Clement, T. P.: Analytical solutions for sequentially coupled one-
569 dimensional reactive transport problems - Part II: Special cases, implementation
570 and testing, *Adv. Water Resour.*, 31, 219–232, 2008b.
- 571 Sudicky, E. A., Hwang, H. T., Illman, W. A., and Wu, Y. S.: A semi-analytical solution
572 for simulating contaminant transport subject to chain-decay reactions, *J. Contam.*
573 *Hydrol.*, 144, 20–45, 2013.
- 574 Sun, Y. and Clement, T. P.: A decomposition method for solving coupled multi-species
575 reactive transport problems, *Transport Porous Med.*, 37, 327–346, 1999.
- 576 Sun, Y., Peterson, J. N., and Clement, T. P.: A new analytical solution for multiple
577 species reactive transport in multiple dimensions, *J. Contam. Hydrol.*, 35, 429–
578 440, 1999a.
- 579 Sun, Y., Petersen, J. N., Clement, T. P., and Skeen, R. S.: Development of analytical
580 solutions for multi-species transport with serial and parallel reactions, *Water*
581 *Resour. Res.*, 35, 185–190, 1999b.
- 582 van Genuchten, M., Wierenga, P. J.: Mass transfer studies in sorbing porous media, I,



583 Analytical solution, *Soil Sci. Soc. Am. J.*, 40, 473-479, 1976.

584 van Genuchten, M.Th., and Parker, J.C.: Boundary conditions for displacement
585 experiments through short laboratory soil columns. *Soil Sci. Soc. Am. J.* 48, 703-
586 708, 1974.

587 van Genuchten, M. T. and Alves, W. J.: Analytical solutions of the one-dimensional
588 convective-dispersive solute transport equation, US Department of Agriculture
589 Technical Bulletin No. 1661, 151 pp., 1982.

590 van Genuchten, M. T.: Convective–dispersive transport of solutes involved in
591 sequential first-order decay reactions, *Comput. Geosci.*, 11, 129-147, 1985.

592 Yeh, G. T.: AT123D: Analytical Transient One-, Two-, and Three- Dimensional
593 Simulation of Waste Transport in the Aquifer System, ORNL-5602, Oak Ridge
594 National Laboratory, 1981.

595 Zhan, H., Wen, Z. and Gao, G.: An analytical solution of two-dimensional reactive
596 solute transport in an aquifer-aquitard system, *Water Resour. Res.*, 45, W10501,
597 doi:10.1029/2008WR007479, 2009.

598

599

600

601

602

603

604

605

606



607 **Table 1. The descriptive simulation conditions and transport parameters**

Parameter	Value
Domain length, L [m]	330.7
Seepage velocity, v [m year ⁻¹]	34.0
Dispersion coefficient, D [m ² year ⁻¹]	1,000
Bulk dry density of the solid grain, ρ_b [kg L ⁻¹]	1.6
Effective porosity, θ [-]	0.2
Distribution coefficient, K_i [L kg ⁻¹]	
PCE	0.784
TCE	0.239
DCE	0.230
VC	0.0545
ETH	0.556
Retardation factor, R_i [-]	
PCE	7.27
TCE	2.91
DCE	2.84
VC	1.44
ETH	5.45
Sorption reaction rate constant, β_i [year ⁻¹]	
PCE	0.5
TCE	0.5
DCE	0.5
VC	0.5
ETH	0.5
Decay constant, λ_i [year ⁻¹]	
PCE	2
TCE	1
DCE	0.7
VC	0.4
ETH	0
Source concentration, $c_{i,0}$ [mg/L]	
PCE	0.056
TCE	15.8
DCE	98.5
VC	3.080
ETH	0.030

608

609



610 Table 2. The convergence behaviors from numerical evaluation of the spatial
 611 concentration distributions of the five species for biodegradation of a chlorinated
 612 solvent at $t=10$ years using the derived analytical solution. (M = number of terms
 613 summed for infinite series expansion).

614

PCE				
$Pe=1$				
x [m]	$N=10$	$N=20$	$N=40$	$N=80$
0	1.15×10^{-2}	1.15×10^{-2}	1.15×10^{-2}	1.15×10^{-2}
82.7	3.88×10^{-3}	3.88×10^{-3}	3.89×10^{-3}	3.89×10^{-3}
165.3	1.31×10^{-3}	1.32×10^{-3}	1.32×10^{-3}	1.32×10^{-3}
248	4.71×10^{-4}	4.70×10^{-4}	4.70×10^{-4}	4.70×10^{-4}
330.7	2.69×10^{-4}	2.66×10^{-4}	2.66×10^{-4}	2.66×10^{-4}
$Pe=10$				
x [m]	$N=250$	$N=500$	$N=1,000$	$N=2,000$
0	2.86×10^{-2}	2.86×10^{-2}	2.86×10^{-2}	2.86×10^{-2}
82.7	1.92×10^{-3}	1.92×10^{-3}	1.92×10^{-3}	1.92×10^{-3}
165.3	1.27×10^{-4}	1.27×10^{-4}	1.27×10^{-4}	1.27×10^{-4}
248	8.38×10^{-6}	8.37×10^{-6}	8.37×10^{-6}	8.37×10^{-6}
330.7	9.22×10^{-7}	8.20×10^{-7}	8.13×10^{-7}	8.13×10^{-7}
$Pe=20$				
x [m]	$N=4,000$	$N=8,000$	$N=16,000$	$N=32,000$
0	3.52×10^{-2}	3.52×10^{-2}	3.52×10^{-2}	3.52×10^{-2}
82.7	1.26×10^{-3}	1.26×10^{-3}	1.26×10^{-3}	1.26×10^{-3}
165.3	4.43×10^{-5}	4.43×10^{-5}	4.43×10^{-5}	4.43×10^{-5}
248	1.53×10^{-6}	1.53×10^{-6}	1.53×10^{-6}	1.53×10^{-6}
330.7	7.30×10^{-8}	7.13×10^{-8}	7.12×10^{-8}	7.12×10^{-8}

615

616

617

618

619

620

621



622

TCE				
<i>Pe=1</i>				
<i>x</i> [m]	<i>N</i> =5	<i>N</i> =10	<i>N</i> =20	<i>N</i> =40
0	4.41×10^0	4.40×10^0	4.40×10^0	4.40×10^0
82.7	2.12×10^0	2.12×10^0	2.12×10^0	2.12×10^0
165.3	1.03×10^0	1.03×10^0	1.03×10^0	1.03×10^0
248	5.47×10^{-1}	5.41×10^{-1}	5.41×10^{-1}	5.41×10^{-1}
330.7	3.87×10^{-1}	3.95×10^{-1}	3.94×10^{-1}	3.94×10^{-1}
<i>Pe=10</i>				
<i>x</i> [m]	<i>N</i> =80	<i>N</i> =160	<i>N</i> =320	<i>N</i> =640
0	9.96×10^0	9.96×10^0	9.96×10^0	9.96×10^0
82.7	1.88×10^0	1.88×10^0	1.88×10^0	1.88×10^0
165.3	3.42×10^{-1}	3.42×10^{-1}	3.42×10^{-1}	3.42×10^{-1}
248	6.04×10^{-2}	6.00×10^{-2}	6.00×10^{-2}	6.00×10^{-2}
330.7	1.55×10^{-2}	1.42×10^{-2}	1.40×10^{-2}	1.40×10^{-2}
<i>Pe=20</i>				
<i>x</i> [m]	<i>N</i> =500	<i>N</i> =1,000	<i>N</i> =2,000	<i>N</i> =4,000
0	1.17×10^1	1.17×10^1	1.17×10^1	1.17×10^1
82.7	1.64×10^0	1.64×10^0	1.64×10^0	1.64×10^0
165.3	2.15×10^{-1}	2.15×10^{-1}	2.15×10^{-1}	2.15×10^{-1}
248	2.64×10^{-2}	2.64×10^{-2}	2.64×10^{-2}	2.64×10^{-2}
330.7	4.93×10^{-3}	3.96×10^{-3}	3.89×10^{-3}	3.89×10^{-3}

623

624

625

626

627

628

629

630

631

632

633

634

635



636

DCE				
<i>Pe=1</i>				
<i>x</i> [m]	<i>N</i> =4	<i>N</i> =8	<i>N</i> =16	<i>N</i> =32
0	3.35×10^1	3.34×10^1	3.34×10^1	3.34×10^1
82.7	1.91×10^1	1.92×10^1	1.92×10^1	1.92×10^1
165.3	1.12×10^1	1.11×10^1	1.11×10^1	1.11×10^1
248	6.84×10^0	6.91×10^0	6.90×10^0	6.90×10^0
330.7	5.61×10^0	5.54×10^0	5.54×10^0	5.54×10^0
<i>Pe=10</i>				
<i>x</i> [m]	<i>N</i> =40	<i>N</i> =80	<i>N</i> =160	<i>N</i> =320
0	7.03×10^1	7.03×10^1	7.03×10^1	7.03×10^1
82.7	2.14×10^1	2.14×10^1	2.14×10^1	2.14×10^1
165.3	5.93×10^0	5.93×10^0	5.93×10^0	5.93×10^0
248	1.55×10^0	1.53×10^0	1.53×10^0	1.53×10^0
330.7	5.76×10^{-1}	4.97×10^{-1}	4.92×10^{-1}	4.92×10^{-1}
<i>Pe=20</i>				
<i>x</i> [m]	<i>N</i> =250	<i>N</i> =500	<i>N</i> =1,000	<i>N</i> =2,000
0	8.03×10^1	8.03×10^1	8.03×10^1	8.03×10^1
82.7	2.05×10^1	2.05×10^1	2.05×10^1	2.05×10^1
165.3	4.54×10^0	4.54×10^0	4.54×10^0	4.54×10^0
248	8.96×10^{-1}	8.94×10^{-1}	8.94×10^{-1}	8.94×10^{-1}
330.7	2.55×10^{-1}	2.00×10^{-1}	1.96×10^{-1}	1.96×10^{-1}

637

638

639

640

641

642

643

644

645

646

647

648

649



650

VC				
<i>Pe=1</i>				
<i>x</i> [m]	<i>N</i> =2	<i>N</i> =4	<i>N</i> =8	<i>N</i> =16
0	1.86×10^1	1.94×10^1	1.96×10^1	1.96×10^1
82.7	2.11×10^1	2.10×10^1	2.09×10^1	2.09×10^1
165.3	1.97×10^1	1.88×10^1	1.89×10^1	1.89×10^1
248	1.63×10^1	1.66×10^1	1.65×10^1	1.65×10^1
330.7	1.45×10^1	1.54×10^1	1.55×10^1	1.55×10^1
<i>Pe=10</i>				
<i>x</i> [m]	<i>N</i> =20	<i>N</i> =40	<i>N</i> =80	<i>N</i> =160
0	2.19×10^1	2.19×10^1	2.20×10^1	2.20×10^1
82.7	3.57×10^1	3.56×10^1	3.56×10^1	3.56×10^1
165.3	2.21×10^1	2.22×10^1	2.22×10^1	2.22×10^1
248	1.09×10^1	1.05×10^1	1.06×10^1	1.06×10^1
330.7	3.80×10^1	5.22×10^1	5.31×10^1	5.31×10^1
<i>Pe=20</i>				
<i>x</i> [m]	<i>N</i> =200	<i>N</i> =400	<i>N</i> =800	<i>N</i> =1,600
0	1.79×10^1	1.79×10^1	1.79×10^1	1.79×10^1
82.7	3.95×10^1	3.95×10^1	3.95×10^1	3.95×10^1
165.3	2.23×10^1	2.23×10^1	2.23×10^1	2.23×10^1
248	8.93×10^0	8.94×10^0	8.94×10^0	8.94×10^0
330.7	3.12×10^0	3.27×10^0	3.28×10^0	3.28×10^0

651

652

653

654

655

656

657

658

659

660

661

662

663



664

ETH				
<i>Pe=1</i>				
<i>x</i> [m]	<i>N</i> =2	<i>N</i> =4	<i>N</i> =8	<i>N</i> =16
0	1.48×10^1	1.49×10^1	1.49×10^1	1.49×10^1
82.7	1.82×10^1	1.82×10^1	1.82×10^1	1.82×10^1
165.3	2.00×10^1	1.99×10^1	1.99×10^1	1.99×10^1
248	2.05×10^1	2.06×10^1	2.05×10^1	2.05×10^1
330.7	2.05×10^1	2.07×10^1	2.07×10^1	2.07×10^1
<i>Pe=10</i>				
<i>x</i> [m]	<i>N</i> =5	<i>N</i> =10	<i>N</i> =20	<i>N</i> =40
0	7.49×10^0	7.84×10^0	7.87×10^0	7.87×10^0
82.7	2.82×10^1	2.78×10^1	2.78×10^1	2.78×10^1
165.3	3.31×10^1	3.20×10^1	3.19×10^1	3.19×10^1
248	1.56×10^1	2.44×10^1	2.46×10^1	2.46×10^1
330.7	5.19×10^1	1.59×10^1	1.73×10^1	1.73×10^1
<i>Pe=20</i>				
<i>x</i> [m]	<i>N</i> =25	<i>N</i> =50	<i>N</i> =100	<i>N</i> =200
0	4.11×10^0	4.12×10^0	4.12×10^0	4.12×10^0
82.7	3.01×10^1	3.01×10^1	3.01×10^1	3.01×10^1
165.3	3.62×10^1	3.62×10^1	3.62×10^1	3.62×10^1
248	2.73×10^1	2.59×10^1	2.60×10^1	2.60×10^1
330.7	3.58×10^1	1.38×10^1	1.47×10^1	1.47×10^1

665

666

667

668

669

670

671

672

673



674 **Figure Captions**

675 Figure 1. Effect of the sorption rate constant on the spatial concentration distribution of
676 species1 at $t=1$ day obtained from the derived rate-limited sorption model. The solid
677 lines are the results from the rate-limited model and the circles represent the results
678 from the equilibrium-controlled sorption model

679 Figure 2. Effect of the inlet boundary conditions on the spatial concentration
680 distribution of species1 at $t=1$ day using different dispersion coefficients.

681

682

683

684

685

686

687

688

689

690

691

692

693

694

695

696

697

698

699

700

701

702

703

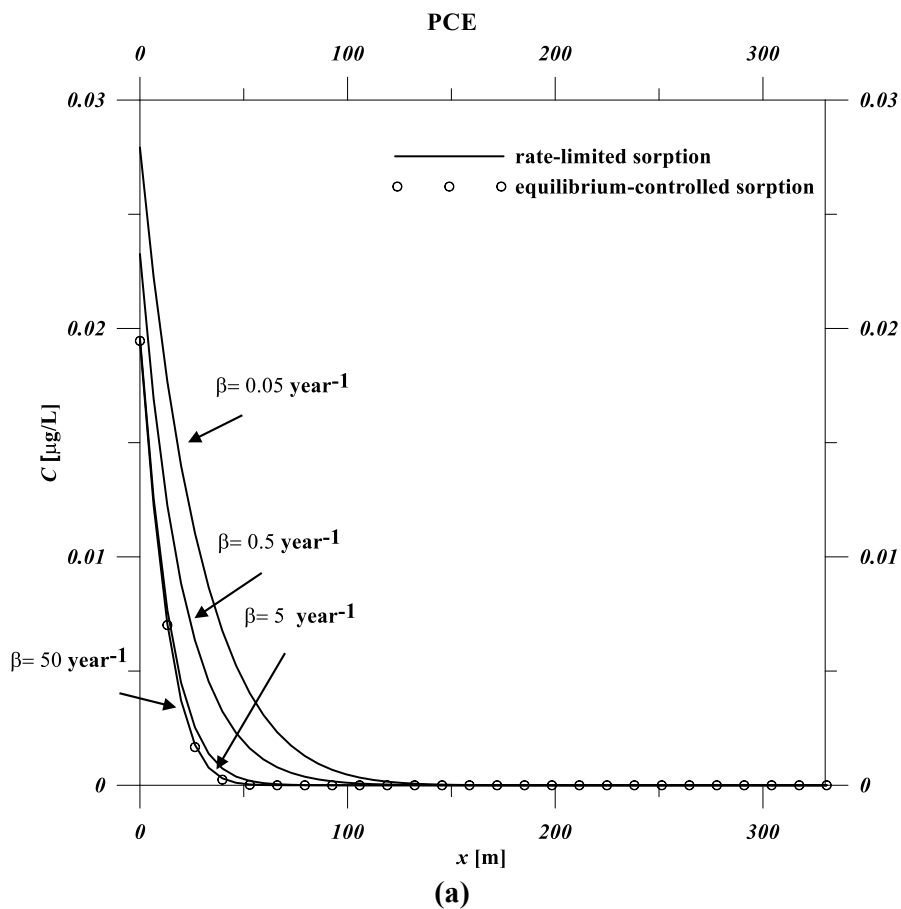
704

705

706



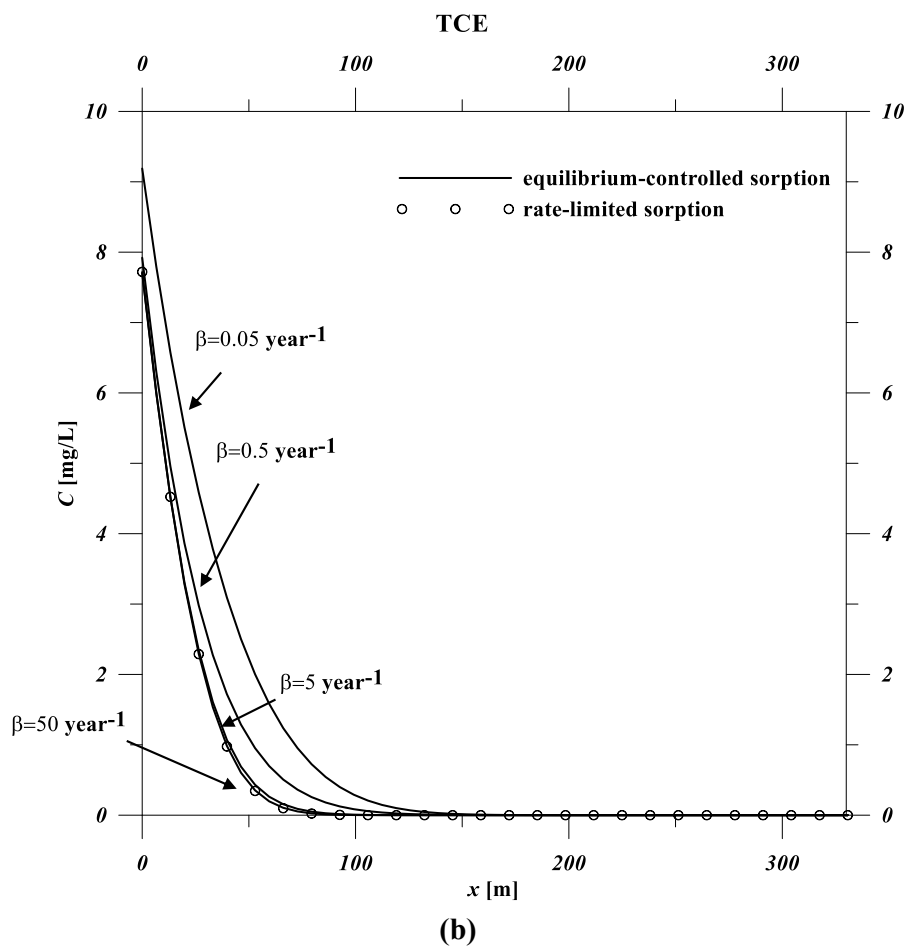
707
708
709



710
711
712
713
714
715
716
717
718
719
720
721



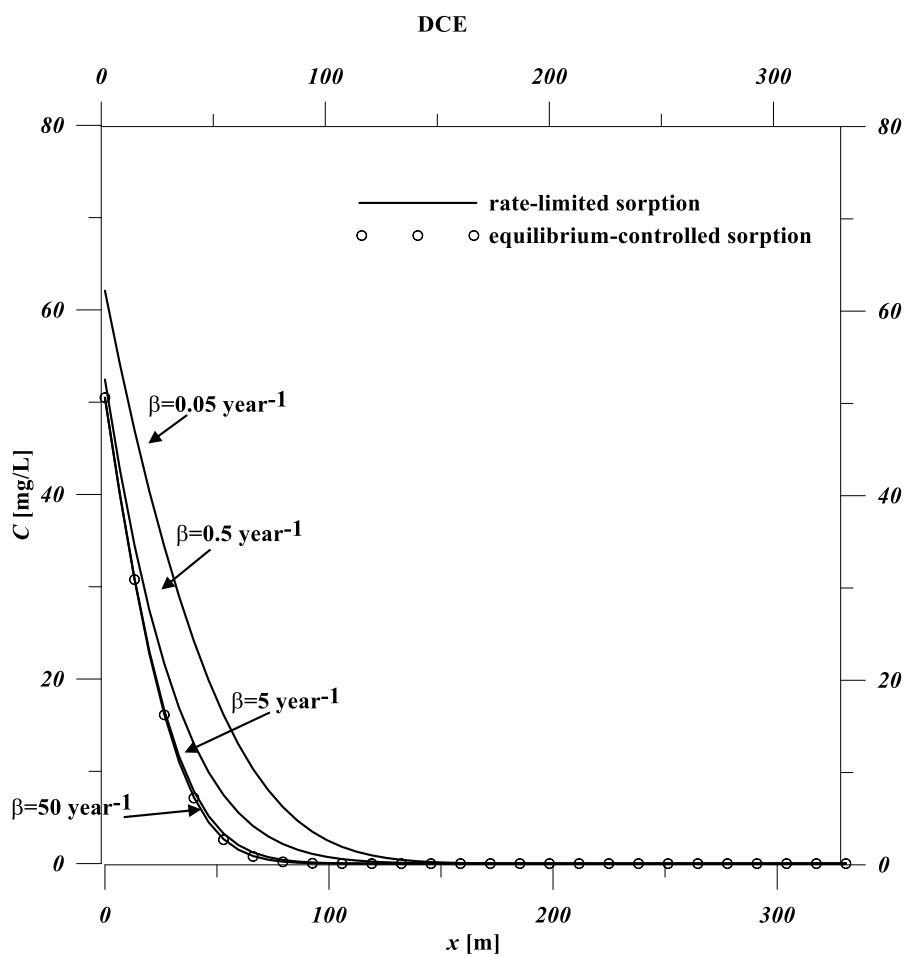
722
723
724



725
726
727
728
729
730
731
732
733
734
735



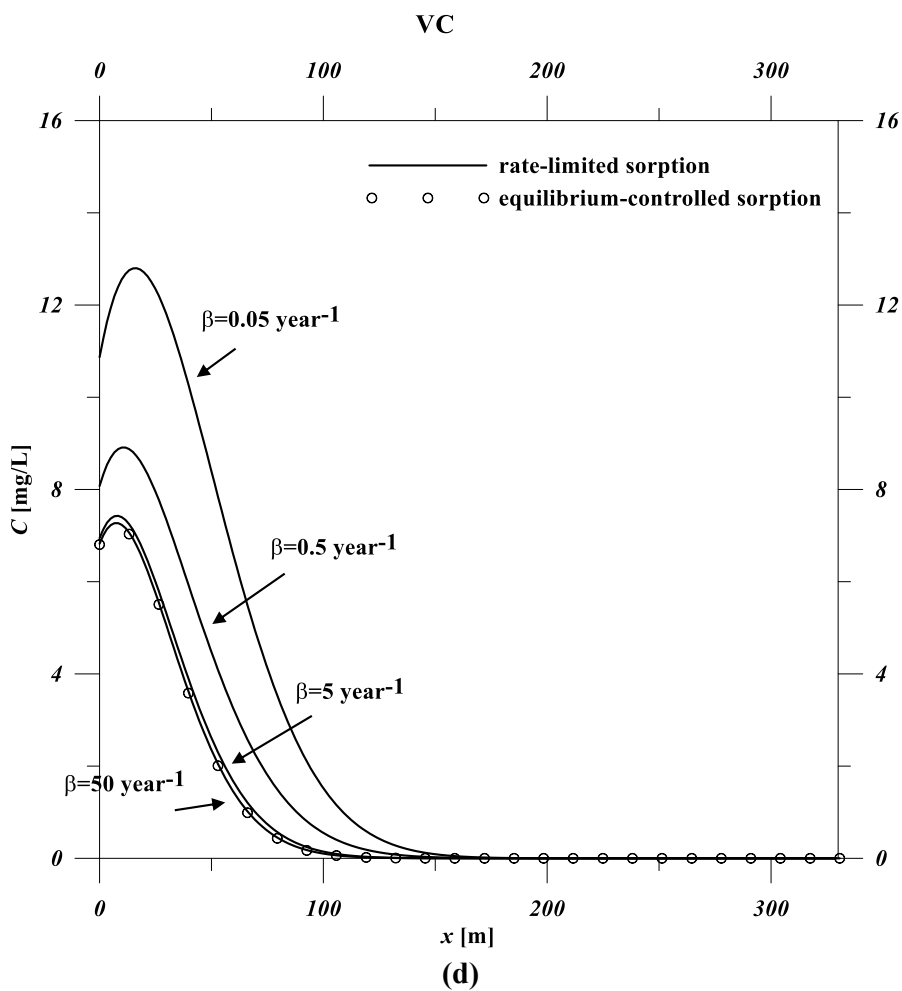
736
737
738



739
740
741
742
743
744
745
746
747



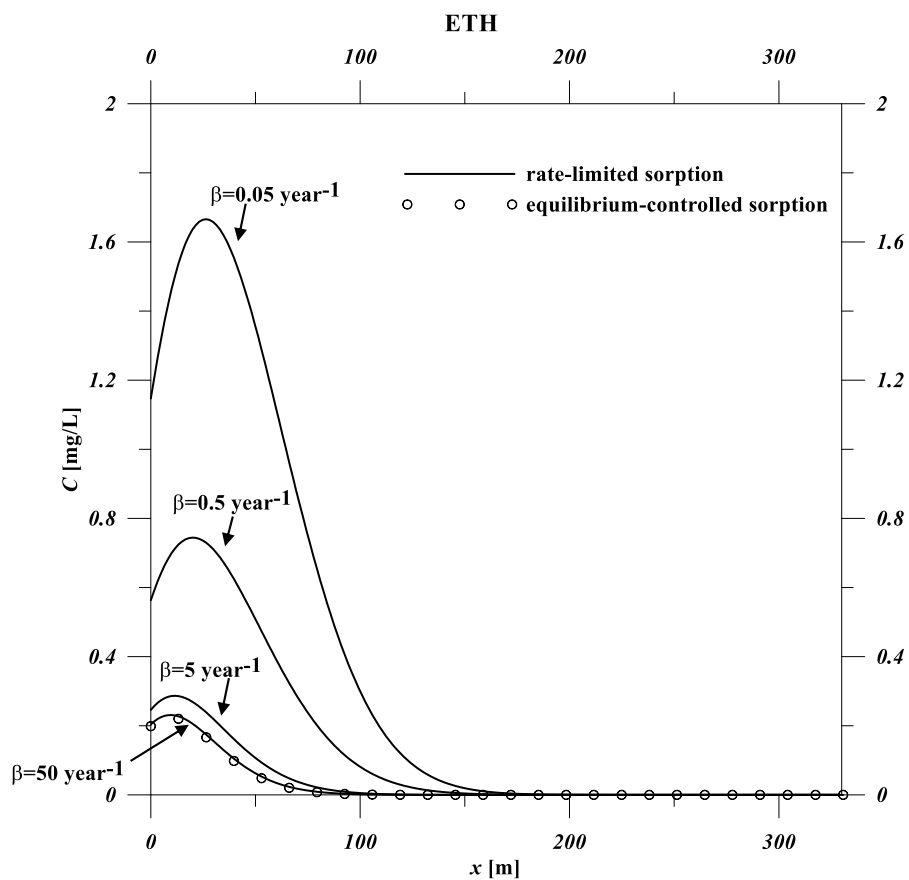
748
749
750
751



752
753
754
755
756
757
758
759
760



761
762
763

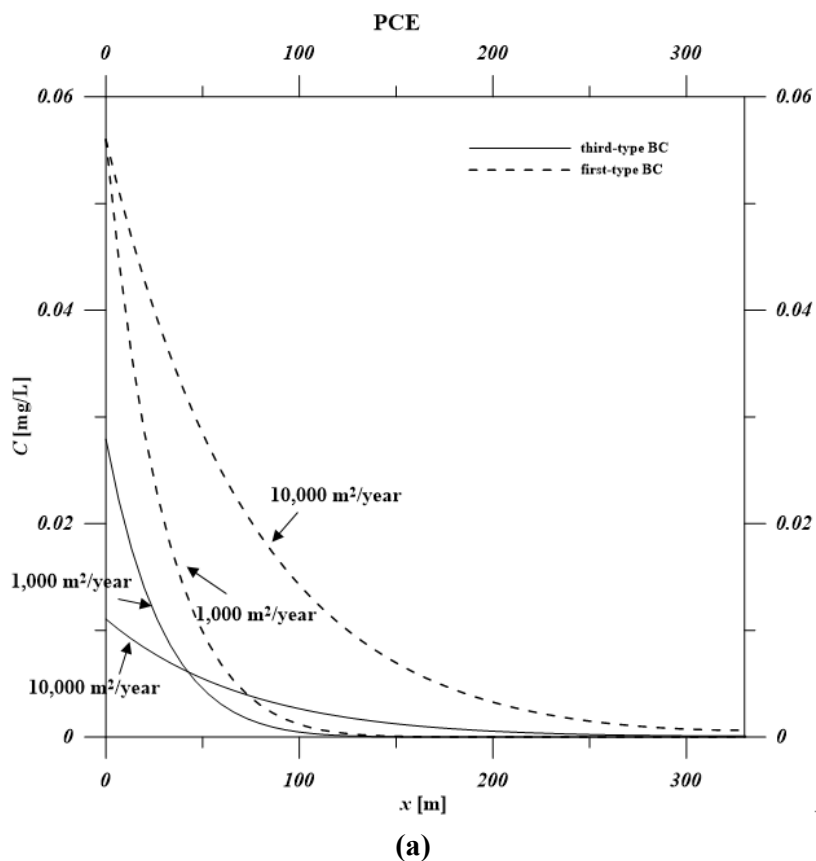


764
765
766
767
768
769
770
771
772
773
774

(e)
Fig. 1



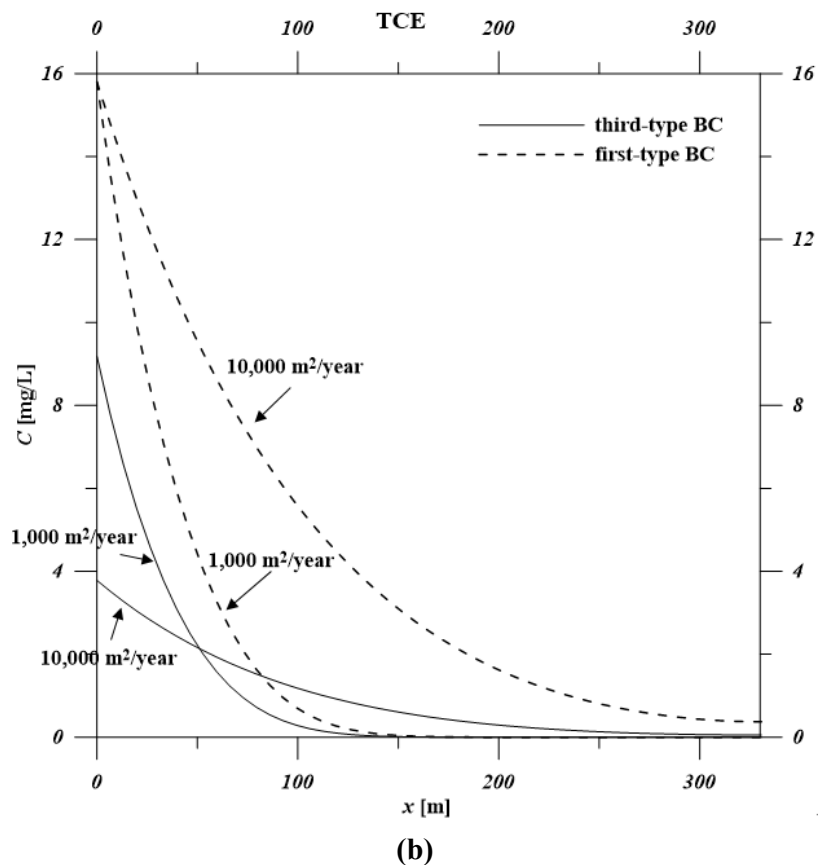
775
776
777



778
779
780
781
782
783
784
785
786
787
788
789
790



791
792
793



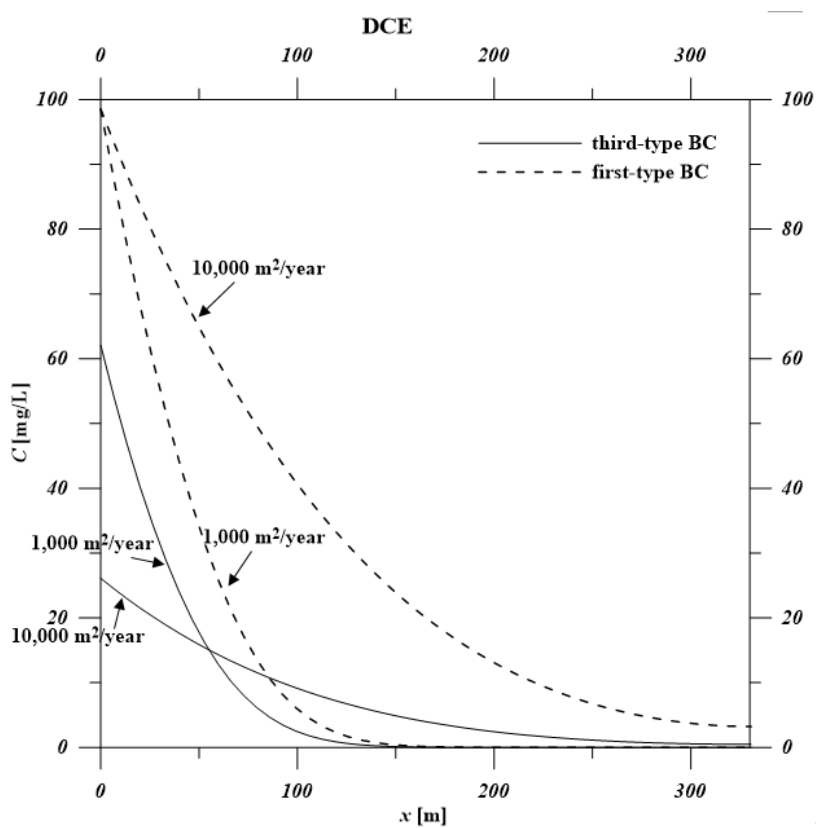
794
795
796
797
798
799
800
801
802
803



804

805

806



807

808

809

810

811

812

813

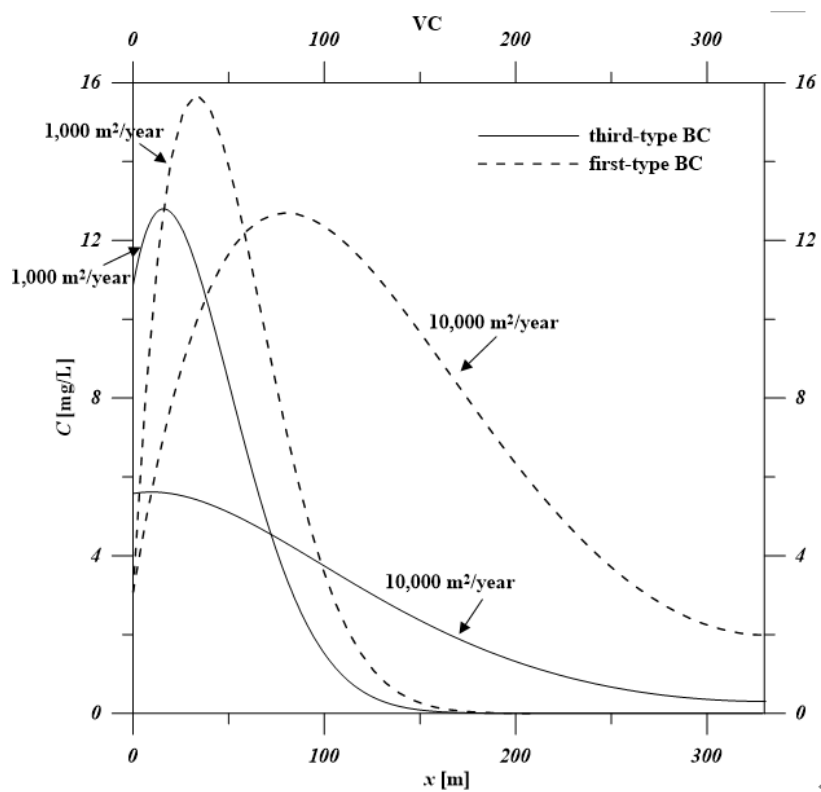
(c)



814

815

816



817

818

819

820

821

822

823

824

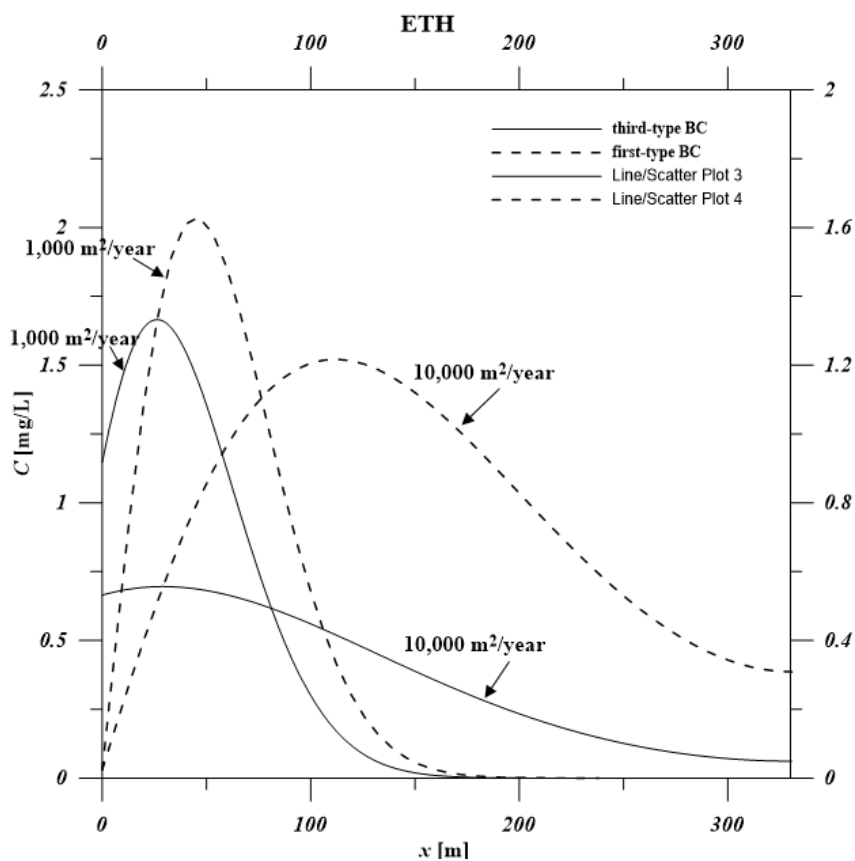
(d)



825

826

827



828

829

830

831

832

(e)
Fig. 2